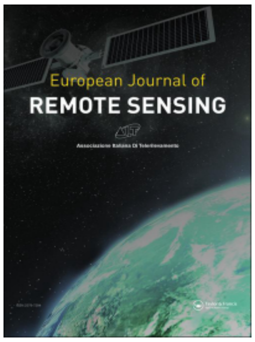

Taylor & Francis
Taylor & Francis Group

European Journal of Remote Sensing

ISSN: 2279-7254 (Online) Journal homepage: www.tandfonline.com/journals/tejr20

Remotely piloted aircraft system and machine learning for detection of coffee plants subjected to foliar application of chitosan

Nicole Lopes Bento, Gabriel Araújo e Silva Ferraz, Mirian De Lourdes Oliveira, Alisson André Vicente Campos, Milene Alves de Figueiredo Carvalho, Dalyse Toledo Castanheira, Ana Cristina de Souza, Tulio de Paula Pires, Giuseppe Rossi & Valentina Becciolini

To cite this article: Nicole Lopes Bento, Gabriel Araújo e Silva Ferraz, Mirian De Lourdes Oliveira, Alisson André Vicente Campos, Milene Alves de Figueiredo Carvalho, Dalyse Toledo Castanheira, Ana Cristina de Souza, Tulio de Paula Pires, Giuseppe Rossi & Valentina Becciolini (2025) Remotely piloted aircraft system and machine learning for detection of coffee plants subjected to foliar application of chitosan, European Journal of Remote Sensing, 58:1, 2476632, DOI: 10.1080/22797254.2025.2476632

To link to this article: https://doi.org/10.1080/22797254.2025.2476632

Published online: 11 Mar 2025.

EUROPEAN JOURNAL OF REMOTE SENSING
2025, VOL. 58, NO. 1, 2476632
https://doi.org/10.1080/22797254.2025.2476632

Taylor & Francis
Taylor & Francis Group

OPEN ACCESS Check for updates

Remotely piloted aircraft system and machine learning for detection of coffee plants subjected to foliar application of chitosan

Nicole Lopes Bento[a], Gabriel Araújo e Silva Ferraz[a], Mirian De Lourdes Oliveira[a], Alisson André Vicente Campos[b], Milene Alves de Figueiredo Carvalho[c], Dalyse Toledo Castanheira[b], Ana Cristina de Souza[b], Tulio de Paula Pires[b], Giuseppe Rossi[d] and Valentina Becciolini[d]

[a]Department of Agricultural Engineering (DEA), School of Engineering (EENG), Federal University of Lavras - UFLA, Lavras, MG, Brazil; [b]Department of Agriculture (DEA), Federal University of Lavras - UFLA, Lavras, MG, Brazil; [c]Department of Agricultural Engineering (DEA), Embrapa Café, Distrito Federal, Lavras, MG, Brazil; [d]Department of Agriculture, Food, Environment and Forestry (DAGRI), University of Florence, Florence, Italy

ABSTRACT
Considered a biostimulant, chitosan can affect the physiological responses of plants to water deficit, acting as an antitranspirant under agricultural stress. Currently, images obtained by Remotely Piloted Aircraft Systems (RPAS), together with machine learning techniques, aid in resolving agricultural problems, including water issues. Therefore, the objective of this study was to differentiate between coffee plants subjected to the foliar application of chitosan and those not subjected to it, based on spectral data extracted from RPAS-acquired images and classification via machine learning. For this purpose, the random forest (RF) classifier was applied to two coffee cultivars (Catucaí Amarelo 2SL and Catuaí Vermelho IAC 99) over two years of study (2021 and 2022). The images were obtained by a 3DR SOLO aircraft with a Parrot Sequoia sensor, processed in PIX4D Mapper software and analysed in QGIS and RStudio software. The results showed good performance metrics for differentiating between coffee plants subjected and not subjected to the foliar application of chitosan, indicating that this method is a valid approach for modelling the presence of the biostimulant in coffee plants, thus confirming that the model can efficiently support the practices of precision agriculture.

ARTICLE HISTORY
Received 19 April 2024
Revised 16 November 2024
Accepted 3 March 2025

KEYWORDS
Digital agriculture; multispectral images; precision coffee growing; remote sensing

Introduction

Chitosan is a substance with high biotechnological potential derived from the process of partial deacetylation of chitin (considered the second most abundant polymer in nature, after cellulose) present in large amounts in the exoskeletons of crustaceans, insects, and fungal cell walls (Huq et al., 2022). In turn, several properties inherent to materials of renewable origin, such as nontoxicity, nonallergy, biocompatibility, biodegradability, analgesic and coagulant properties, and antimicrobial action against fungi and bacteria, enable its application in biological systems (Pellá et al., 2018).

Chitosan has several characteristics that make it suitable for use in different applications, especially agricultural and environmental applications. Some of the applications include pesticides, herbicides, insecticides, fertilizers, soil conditioning agents, plant disease control agents, antitranspirants, biostimulants and seed and nutrient coatings (Cheng et al., 2017; Kumaraswamy et al., 2018). It also promotes numerous defense responses related to biotic and abiotic stresses, especially in the protection of plants against environmental stress. In plants, chitosan improves drought tolerance in plants by stimulating their physiological responses to water deficit, suggesting the potential of this biopolymer to act as an antitranspirant in agricultural situations of water deficit. Drought tolerance is induced via increased water use efficiency and greater defense against oxidative stress (Hidangmayum et al., 2019). Thus, when applied topically, chitosan improves stomatal conductance, increases the abscisic acid content and reduces transpiration in plants without changing their height, leaf area, root or biomass (Román-Doval et al., 2023).

Agricultural studies on the use of chitosan have already demonstrated its ability to delay or prevent the spread of diseases, fungi, bacteria and viruses and to increase and stimulate the defense mechanisms of plants, such as beans (Abd El-Aziz & Khalil, 2020), cucumber (Gangireddygari et al., 2021), rice (Liu et al., 2012), sweet potato (Xing et al., 2018), pear (Meng et al., 2020), strawberry (Feliziani et al., 2015), grapevine (Reglinski et al., 2010), dragon fruit (Zahid et al., 2015), wheat (Masjedi et al., 2017), barley (Behboudi et al. 2018, Behboudi et al., 2018), sugarcane (Silveira et al., 2019), and others. However, in the context of coffee cultivation, there are few studies with the direct application of chitosan. The significance of this crop is

CONTACT Gabriel Araújo e Silva Ferraz gabriel.ferraz@ufla.br Department of Agricultural Engineering (DEA), School of Engineering (EENG), Federal University of Lavras - UFLA, Aquenta Sol, 3037 Lavras- Minas Gerais, Brazil

the enormous contribution to the world economy since Brazil is the largest producer and exporter of coffee in the world (Companhia Nacional de Abastecimento - CONAB, 2023). As such, given the needs described for coffee crops, the applicability of chitosan as a form of agricultural management is addressed, allowing us to circumvent the physiological and morphological disturbances that affect the development and yield of coffee crops.

Thus, the use of techniques and technologies that demonstrate the responses of plants in the field allows for the accurate study of agricultural crops, intelligent decision making and increased profitability (Bento et al., 2022). The use of suborbital remote sensing with Remotely Piloted Aircraft Systems (RPAS) is recommended because they allow aerial imaging closer to the surface, ensuring greater spectral resolution, as well as the use of multispectral sensors, which ensure greater resolution of radiometric measurement and may also target smaller study areas, ensuring lower costs (Santos et al., 2020). RPAs are defined in summary as remotely piloted aircraft operated through interfaces such as computers, simulators, digital devices, or remote controls, with the pilot not being on board (Santos et al., 2020).

In recent years, the use of products obtained by RPAS combined with machine learning techniques has introduced a new way of examining various sets of data serving different areas, such as precision agriculture (Calou et al., 2020). Machine learning allows solving nonlinear issues by employing datasets from various sources and exposing hidden information in the data initially provided (Liakos et al., 2018; Qiu et al., 2016). The use of different computational algorithms allows the generalization of patterns, allowing robust and flexible prediction models to be developed for increasingly diverse study objectives (Priya & Ramesh, 2020).

In the context of precision coffee farming, machine learning techniques have been used to study plant diseases (Marin, Ferraz, Santana, et al., 2021), productivity (Barbosa et al., 2021; Kouadio et al., 2018), leaf nitrogen (Marin, Ferraz, Guimarães, et al., 2021), identification and counting of plants (Santana et al., 2023) and weeds (Bento et al., 2023). However, the use of chitosan in the study of coffee plants subjected to foliar management has not yet been discussed in the literature, which is a gap that demands attention and directs new promising results of applicability. Therefore, this study aimed to evaluate the potential use of multispectral images obtained by RPAS together with the use of machine learning techniques to differentiate coffee plants subjected and not subjected to the foliar application of chitosan.

Identifying plants that respond positively to the application of chitosan can lead to more precise adjustments in agricultural management. Plants treated with biostimulants such as chitosan tend to exhibit improvements in growth, root development, and photosynthesis, resulting in increased productivity. For coffee growers, this practice can translate into higher crop yields and better grain quality, directly impacting profits. Moreover, this approach simplifies the monitoring of established trials, enabling more consistent assessments of plant responses and facilitating long-term agricultural planning. The application of chitosan as it is a less invasive method, compared to the use of synthetic fertilizers or pesticides, generates a positive impact on the plants, which in turn benefits the soil, biodiversity, and agricultural ecosystems, while also meeting the growing demand for more sustainable agricultural practices.

Materials and methods

Study area

The study area refers to a commercial coffee crop (Coffea arabica L.) located in the municipality of Ijaci, Minas Gerais, Brazil (501,780 and 502,320 m E and 7,659,700 and 7,659,140 m N), in the projection system Universal Transverse Mercator (UTM), 23S zone, SIRGAS 2000 (Figure 1). The crop was planted in 2008 and has a spacing of 3.6 metres between rows and 0.5 metres between plants, with two different cultivars, Catucaí Amarelo (2SL) (subarea A) and Catuaí Vermelho (IAC 99) (subarea B), registered in the National Register of Cultivars – RNC, of the Ministry of Agriculture, Livestock and Food Supply – Mapa.

The experimental design consisted of randomized blocks, with different foliar application treatments (with/without chitosan) (Figure 1). The division consists of two study lines per coffee cultivar, with 8 blocks per study line, 4 blocks subjected to chitosan application and 4 blocks without chitosan application, with 6 replicates per block. Each replicate refers to a study plant; thus, each experimental unit is composed of 8 total plants, with 6 plants being the focus of investigation. The lateral lines of each experimental line were also considered as borders.

The chitosan product that was powdered to prepare the solution (liquid) that was applied, using the commercial active from Sigma Aldrich Chemicals (low molecular weight chitosan 448,869-250 G). Chitosan foliar applications were carried out with an electric knapsack sprayer, totaling three applications in the months of February (23 February 2021), March (30 March 2021) and May (4 May 2021). Chitosan was applied at a concentration of 300 mg.L.-1, solubilized in 0.1% acetic acid, and the dilution of chitosan in acid was carried out on the same day of applications. The volume of mixture used during applications was 400 L.ha.-1, with suitable climatic conditions for the application.

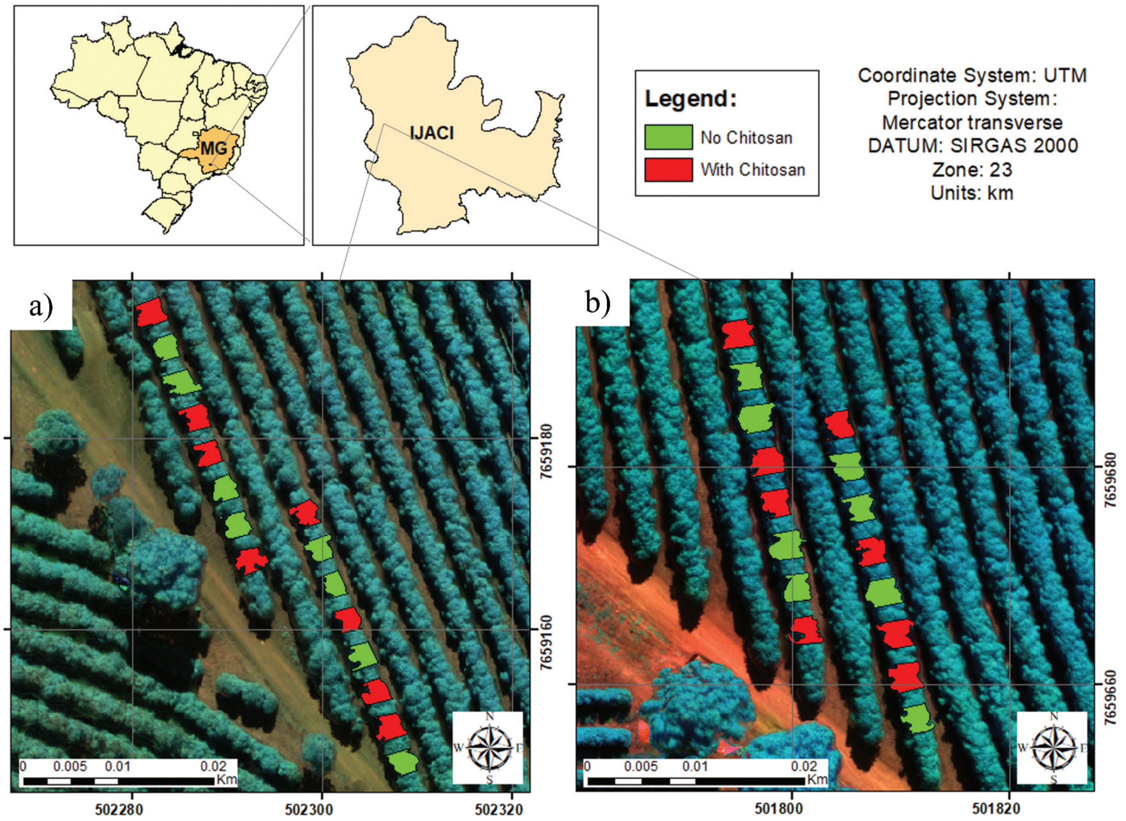

Figure 1. Study area with separation of the subareas for the coffee cultivars (a) catucaí amarelo (2SL) and (b) Catuaí Vermelho (IAC 99).

Collection and processing of air data

Aerial imaging was performed in June 2020 and 2021 using a 3DR SOLO Remotely Piloted Aircraft (3D Robotics, Berkeley, California) (Figure 2a), which, according to the manufacturer's considerations, has a flight autonomy of approximately 20 minutes (considering the weight loaded on the vessel), maximum load capacity of 0.42 kg, maximum altitude of 122 m, range of 800 m and maximum speed of 24.58 m/s with navigation, altitude and other communications control by means of telemetry and in real time with control inputs via the Wi-Fi network.

The Parrot Sequoia multispectral sensor (MicaSense, Seattle, WA, USA) and the irradiance sensor (Sunshine Sensor) were embedded in the RPA for aerial imaging (Figure 2b). This sensor has an RGB reading range and 4 spectral sensors with spectral ranges of green (GRE – 550 to 590 nm), red (RED – 660 to 700 nm), red edge (REG – 735 nm to 745 nm), infrared (NIR – 760 to 820 nm) and RGB (380 to 720 nm), and its dimensions are 47 mm x 39.6 mm x 18.5 mm and the focal aperture is 61.9° HFOV (high-frequency oscillatory ventilation) (4 mm).

The flight plan was developed semiautomatically using Mission Planner software (Team ArduPilot, Geelong, Australia). Regarding the flight parameters, the aircraft launch and landing location (home point definition), wind direction, topographic conditions of the area, flight direction, flight height in metres and flight speed in m/s were considered. The overlap information (overlap X sidelap), speed and flight height above ground level (AGL) were standardized at 80% X 80%, 5 m/s and 40 m, respectively.

Before and after the flights, images were captured from the radiometric calibration plate (MicaSense,

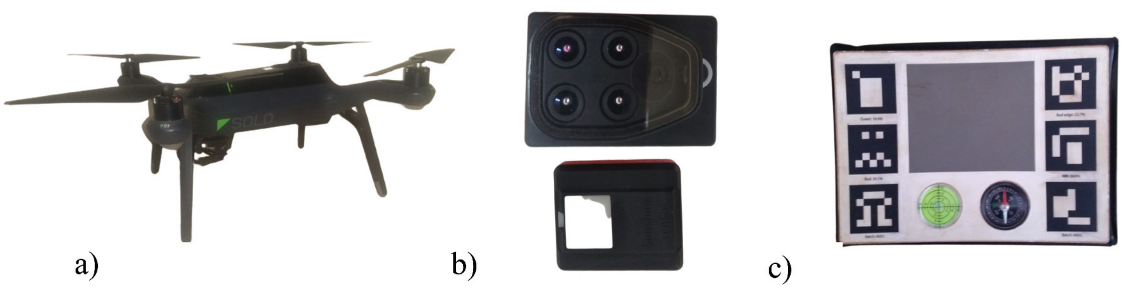

Figure 2. (a) 3DR SOLO RPA; (b) parrot sequoia and sunshine sensor; and (c) radiometric calibration plate.

Seattle, WA, USA) for later standardization of the reflectance values of the flights since the panel has a known reflectance curve and allows for accurate compensation of the incident light (Figure 2c). The flights took place at standardized times between 11:00 am and 1:00 pm, a time that avoids shading of the plants due to the position of the sun at the zenith.

The aerial images were processed using Pix4D Mapper software (Pix4D, Lausanne, Switzerland). The workflow steps refer to the initial alignment of the images through triangulation and creation of link points, subsequently generating the dense point clouds and texture of the scenes, and finally orthorectifying the images to obtain the orthomosaic from the end of each spectral band for each study area and date. The generated orthomosaics had a ground sampling distance (GSD) of 0.052 m.

With the orthomosaic products in hand, the study blocks were individualized using QGIS 3.6.2 software (QGIS Development Team, Open Source Geospatial Foundation), with each experimental unit composed of 6 useful plants, enabling the extraction of the orthomosaic pixel values for each block of plants for the subsequent spectral analyses.

Vegetation indices

The vegetation indices (VIs) were calculated based on the combination of spectral bands according to the mathematical equations described in Table 1. For this study, 26 different VIs were considered for identifying the indirect relationships of spectral response in coffee plants subjected to the different treatments and to serve as input data for the classification model. The VIs was calculated with the software QGIS 3.6.2 (QGIS Development Team, Open Source Geospatial Foundation) in a GIS environment through the set of functions in ArcToolbox in the Map Algebra tool.

Classification and validation

The training and validation stages of the classification model consisted of a) preprocessing and exploratory analysis of the data; b) sampling of classes of interest; c) classification procedure by the random forest (RF) algorithm; d) validation and verification of the performance of the classifier; and e) forecasting in the total area, with steps shown in Figure 3 and procedures performed in QGIS 3.22.8 (QGIS Development Team, Open-Source Geospatial Foundation) and R Studio software (R Development Core Team, R project, Austria, Vienna). In this study, the data referring to the 26 VIs and 4 individual spectral bands of the sensor used to capture the images were considered as input data to the classification process.

Two classes of interest were considered for the classification process: coffee plants subjected to chitosan application (CQ) and coffee plants not subjected to chitosan application (SQ). The training samples were selected based on the sketch of the study area, based on the correct positioning of the plants subjected to the different treatments, using the software QGIS 3.22.8 (QGIS Development Team, Open Source Geospatial Foundation). The samples were initially collected in

Table 1. Vegetation indices used, followed by their abbreviations, equations and references.

Vegetation Indices	Abbreviations	Equations[1]	References
Chlorophyll Index Green	Clg	$((R_{NIR}/R_G -1)$	Gitelson et al. (2003)
Difference Vegetation Index	DVI	$(R_{NIR}+R_R)$	Perry and Lautenschlager (1984)
Excess Red Vegetation Index	EXR	$1.44(R_R-R_G)$	Meyer et al. (1998)
Green Difference Vegetation Index	GDVI	$(R_{NIR}+R_G)$	Wu (2014)
Green Normalized Difference Vegetation Index	GNDVI	$(R_{NIR}-R_G)/(R_{NIR}+R_G)$	Shanahan et al. (2001)
Green Optimal Soil Adjusted Vegetation Index	GOSAVI	$(1 + 0.16)(R_{NIR}-R_G)/(R_{NIR}+R_G +0.16)$	Rondeaux et al. (1996)
Green Re-normalized Different Vegetation Index	GRDVI	$(R_{NIR}-R_G)/\sqrt{}(R_{NIR}+R_G)$	Cao Qiang et al. (2013)
Green Red NDVI	GRNDVI	$(R_{NIR})-(R_G+R_R)/(R_{NIR})+(R_G+R_R)$	Wang et al. (2007)
Green-Red Ratio Index	GRRI	$(R_G)/(R_R)$	Gamon and Surfus (1999)
Green Ratio Vegetation Index	GRVI	(R_{NIR}/R_G)	Tucker (1979)
First Modified Chlorophyll Absorption Ratio Index	MCARI1	$1.2(2.5((R_{NIR}-R_G)-1.3(R_{NIR}-R_G)))$	Haboudane (2004)
Modified Double Difference Index	MDD	$(R_{NIR}-R_{REG})-(R_{REG}-R_G)$	Lu et al. (2017)
Modified Normalized Difference Index	MNDI	$(R_{NIR}-R_{REG})/(R_{NIR}-R_G)$	Cao Qiang et al. (2013)
Modified Photochemical Reflectance Index	MPRI	$(R_G-R_R)/(R_G+R_R)$	Yang et al. (2008)
Modifed Simple Ratio	MSR	$(R_{NIR}/R_R)-1/\sqrt{}(R_{NIR}/R_R)+1$	Chen (1996)
Modified Simple Ratio Green	MSR_G	$(R_{NIR}/R_G)-1/\sqrt{}(R_{NIR}/R_G)+1$	Cao Qiang et al. (2013)
Meris Terrestrial Chlorophyll Index	MTCI	$(R_{NIR}-R_{REG})/(R_{REG}+R_R)$	J. Dash and Curran (2004)
Normalized Different Index	NDI	$(R_G-R_R)/(R_G+R_R +0.01)$	Mao et al. (2003)
Normalized Difference Red Edge Index	NDRE	$(R_{NIR}-R_{REG})/(R_{NIR}+R_{REG})$	Buschmann and Nagel (1993)
Normalized Difference Vegetation Index	NDVI	$(R_{NIR}-R_R)/(R_{NIR}+R_R)$	Rouse et al. (1974)
Normalized Green Index	NGI	$R_G/(R_{NIR} +R_{REG}+R_G)$	Sripada et al. (2006)
Normalized NIR Index	NNIR	$R_{NIR}/(R_{NIR}+R_{REG}+R_G)$	Sripada et al. (2006)
Normalized Red Edge Index	NREI	$R_{REG}/(R_{NIR}+R_{REG}+R_G)$	Cao Qiang et al. (2013)
Normalized Red Index	NRI	$R_R/(R_{NIR}+R_{REG}+R_{RED})$	Bausch and Duke (1996)
Renormalized Difference Vegetation Index	RDVI	$(R_{NIR}-R_R)/\sqrt{}(R_{NIR}+R_R)$	Roujean and Breon (1995)
Ratio Vegetation Index	RVI	R_{NIR}/R_R	Richardson and Wiegand (1977)

Legend: [1] R_{NIR}, reflectance values obtained by the sensor in the near infrared range. R_{REG}, reflectance in the red edge range. R_R, reflectance in the red band. R_G, reflectance in the green band.

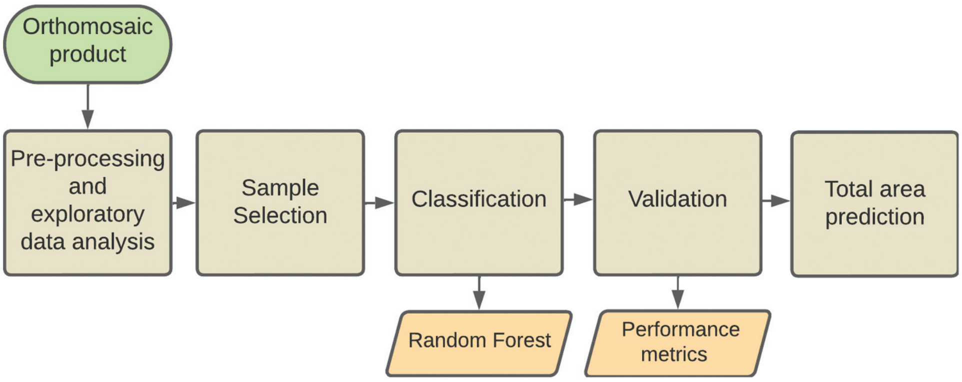

Figure 3. Flowchart of the classification process with the methodological steps used.

shapefile format based on regions of interest (ROIs). The pixels belonging to the ROIs were added as samples, increasing the number of samples, totaling 51,409 samples for the cultivar Catucaí Amarelo (2SL) and 54,942 samples for the cultivar Catuaí Vermelho (IAC 99), using R Studio software (R Development Core Team, R project, New Zealand).

Subsequently, using R Studio software, the samples were randomly divided into training and validation samples at proportions of 70% and 30%, respectively. The training samples were used in the classification for separating information from the reflectance spectrum using the random forest (RF) machine learning algorithm (Breiman, 2001) in R Studio software. For this analysis, the hyperparameters were defined as follows: the number of decision trees (ntree) was set to 100, and the number of variables tested at each split (mtry) was defined as the square root of the total number of input variables (Gislason et al., 2006). Additionally, an analysis based on the Gini index was performed to describe the importance of each input variable for the classification process. The remaining hyperparameters were set to their default values: nodesize = 1 (minimum size of terminal nodes); maxnodes = no defined limit (maximum number of nodes); sampsize = total number of samples in the dataset (sampling size); replace = true (sampling with replacement); proximity = false (proximity matrix not computed); classwt = null (no class weights); and cutoff = 1/number of classes (default cutoff for classification).

The results were validated using the study's percentage of the validation sample in direct comparison to the reference data. For this, we used information obtained through the confusion matrix according to metrics of global accuracy, sensitivity, specificity and area under the ROC curve. Finally, the classifier algorithm was used to predict the total area of the study classes; therefore, it was possible to identify the blocks of coffee plants subjected and not subjected to the foliar application of chitosan.

Results

The performance metrics are described in Table 2 and refer to the overall accuracy, sensitivity, specificity and area under the ROC curve according to the classification proposed by the algorithm for the two coffee cultivars studied, Catucaí Amarelo (2SL) and Catuaí Vermelho (IAC 99), and the results of this analysis consider the study classes in general, considering the two study classes, coffee plants subjected to chitosan application (CQ) and coffee plants not subjected to chitosan application (SQ). In general, satisfactory values of the performance metrics analyzed were found, which indicate good performance of the classifier for differentiating the study classes.

The results of the validation of the classification algorithm for the two coffee classes and cultivars studied were verified using confusion matrices, as described in Table 3. The results of this analysis consider the study classes individually. Based on the values previously presented via performance metrics, the confusion matrix showed low errors between the classified thematic classes, with approximately 18% for SQ and 22% for CQ for the cultivar Catucaí Amarelo (2SL) and 15% for SQ and 22% for cultivar Catuaí Vermelho (IAC 99).

Using the RF classifier, it was possible to describe the importance of each variable for the classification process by means of the mean decrease in the Gini, as shown in Figure 4. For the cultivar Catucaí Amarelo (2SL), the 3 most important variables in the

Table 2. Performance metrics for the RF classification algorithms for the coffee cultivars A) catucaí amarelo (2SL) and B) Catuaí Vermelho (IAC 99).

	Overall Accuracy	Sensitivity	Specificity	AUC
A)	0.8025	0.8230	0.7822	0.8087
B)	0.8169	0.8516	0.7812	0.8237

Table 3. Confusion matrices for the RF machine learning algorithm for the coffee cultivars A) catucaí amarelo (2SL) and B) Catuaí Vermelho (IAC 99).

		Reference		
A)	Classes	SQ	QC	Total
		SQ	QC	Total
Prediction	SQ	6307	1690	7997
	QC	1356	6069	7425
	Total	7663	7759	15422
		Reference		
B)	Classes	SQ	QC	Total
Prediction	SQ	5422	1351	6773
	QC	945	4825	5770
	Total	6367	6176	12543

Legend: SQ - without chitosan; CQ - with chitosan.

classification were the REG spectral band VIs MNDI and NNIR, and for the cultivar Catuaí Vermelho (IAC 99), the 3 most important variables in the classification were VIs MDD, NDRE and the NIR spectral band.

The map of the distribution of classes with the classifier RF, which describes the prediction of classes by the classifier algorithm for the plant blocks of the two coffee cultivars, is presented in Figure 5, where A) Catucaí Amarelo (2SL) and B) Catuaí Vermelho (IAC 99).

Discussion

As shown in Table 2, the performance metrics of overall accuracy, sensitivity, specificity and area under the ROC curve allowed reliable discrimination of the study classes. The global accuracy metric allowed us to verify the estimate of the global correctness ratio of the classifier algorithm, while the sensitivity metric refers to the proportion of true positives among the instances classified as positive, and the specificity metric refers to the proportion of false negatives among the instances classified as negative. Finally, the metric referring to the area under the ROC curve refers to the fit between sensitivity and specificity (De Castro & Ferrari, 2017; Mariano & Paz, 2020).

Notably, values of performance metrics between 70 and 100% represent satisfactory results from moderate to high for classification (Kuhn & Johnson, 2013), as observed in this study, with values always above 78%. For the area under the ROC curve, the performance is represented in the range of normalized limits between 0 and 1 (James et al. 2013, Kuhn & Johnson, 2013). Values closer to 1 highlight better performance, as observed in this study with values above 0.80. Thus, it can be said that all performance metrics are within the quality limits as defined by the classification criteria. It should be noted that pixels classified as erroneous classes are checked whenever the classification does not reach 100% accuracy in the individual analysis of the classes.

The RF algorithm has some specificities that optimize the classification procedures since it calculates the average of the decision trees that compose it, which minimizes the variation component of the model, bringing it closer to an ideal model. When developing trees, independent decisions and obtaining a majority vote reduces the fit errors and increases the correctness of the proposed classes (Mehta et al., 2019), a fact evidenced in this study. In addition, this algorithm can list the attributes that contribute to decision making and is often used as a feature selection technique, a fact considered essential for data analysis because it allows reducing the complexity/dimensionality of the classification system (M. Dash & Liu, 1997). Other characteristics that make RF beneficial to classification applications stand out, such as the lower interference of outliers and data with noise, allowing data with different

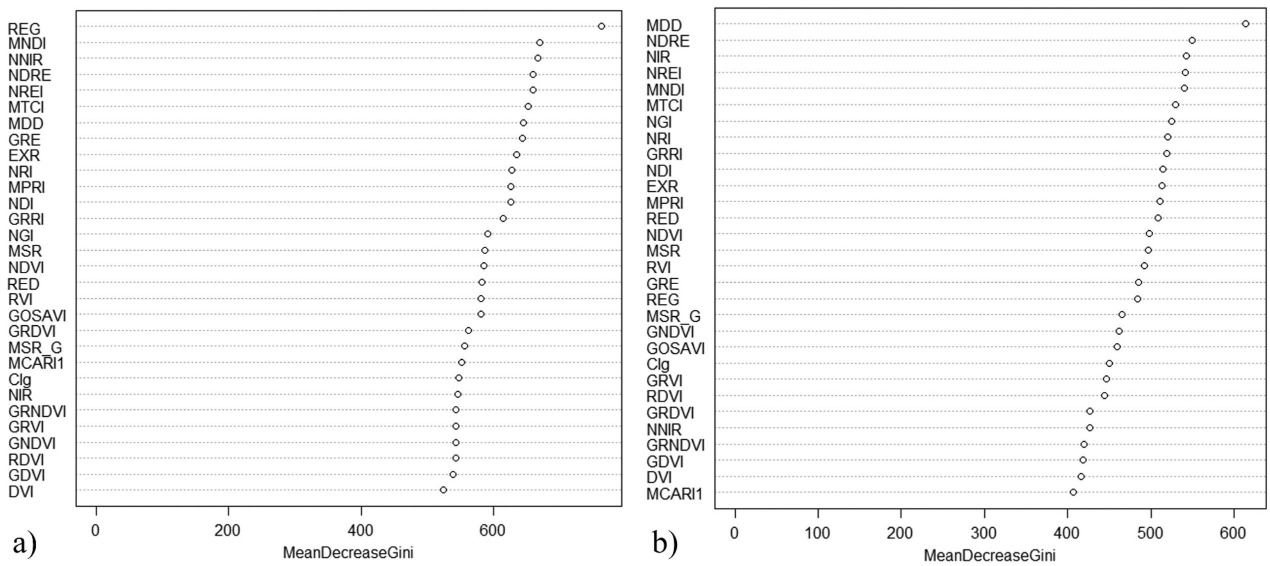

Figure 4. Importance variables by mean decrease in gini in the spectral bands for the coffee cultivars (a) catucaí amarelo (2SL) and (b) Catuaí Vermelho (IAC 99).

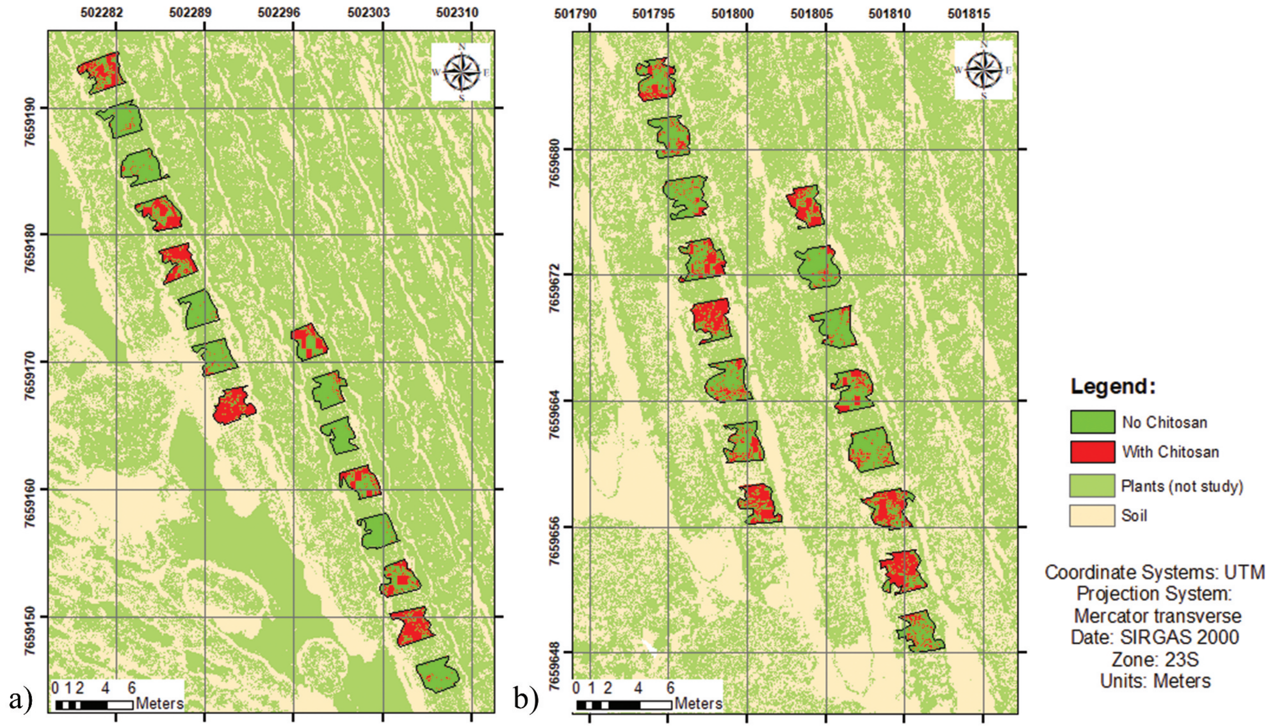

Figure 5. Prediction map with the RF classifier for the blocks of plants subjected and not subjected to foliar application of chitosan for the coffee cultivars (a) catucaí amarelo (2SL) and (b) Catuaí Vermelho (IAC 99).

statistical distributions, large-scale data and data from various sources, along with having higher precision when compared to other classification algorithms such as support vector machine and maximum likelihood (De Almeida Furtado et al., 2016; Mahdianpari et al., 2017).

The RF classification errors observed in this study may be associated with the characteristics of the plants when subjected to foliar application of chitosan and consequently with the reflectances presented in their spectral responses. When chitosan is applied foliar to plants, it promotes changes in the plant's internal structure, producing defense and protection reactions by activating mechanisms of production and/or inhibition of elements and compounds present (Berger et al., 2011). Plants under stress conditions, especially water stress, inhibit the growth of roots and stems and reduce photosynthesis, which may directly affect the leaf size and proportion and consequently changes in the leaf area index (LAI), thus decreasing the uptake and activity in the photosynthetically active area (Xing & Wu 2012) and altering the spectral responses of plants. Therefore, the adoption of antitranspirant methods, especially the foliar application of chitosan, promotes changes in the plant structure, which was captured via spectral analysis and direct application of image classification.

It was observed in this study that in addition to the use of the individual spectral bands of the sensor, the use of VIs demonstrated improvements in the classification procedure, resulting in spectral differences that were captured by the RF algorithm for the analysed study classes. This occurs mainly because the VIs emphasizes characteristics related to biological variables, such as chlorophyll content and biomass, which are important for differentiating the classes of the study. According to Figure 4, for the cultivar Catucaí Amarelo (2SL) in addition to the REG band, the VIs MNDI and NNIR had greater weight in the classification process, and for the cultivar Catuaí Vermelho (IAC 99) in addition to the NIR spectral band, the VIs MDD and NDRE had greater weight in the classification process.

The active presence of the NIR and REG spectral bands are strongly weighted in the proposed classification, whether used individually or in combination according to VIs. The NIR spectral region is influenced mainly by the internal structure of the leaves due to the interaction of incident energy with the structure of the spongy mesophyll of the leaves (Knipling, 1970). The same occurs in the REG spectral region, located in the sensitive interval between the RED and NIR spectral bands (spectral band of low and high reflectance in plants, respectively), allowing the identification of changes in the levels of chlorophyll in the vegetation affected by stress factors imposed by agricultural practices (Barnes et al., 2017; Cao et al., 2019). Thus, it is noteworthy that the water content of vegetation, according to water stress, alters the reflectance in various regions of the electromagnetic spectrum. In this study it was observed especially in the REG and NIR spectral bands, since it promotes significant changes and adaptations of plants, thus affecting its entire functioning, development, and spectral responses, as demonstrated in studies by Le et al. (2023) and Fiorio et al. (2018).

The prediction map presented in Figure 5 describes the distribution of study classes according to the RF classifier, highlighting the fact that the algorithm obtained high accuracy for the proposed classification by correctly identifying the distribution for the blocks of plants subjected and not subjected to foliar application of chitosan. In general, satisfactory and accurate results of the proposed classification are due to the use of high spatial resolution images obtained by RPAS, as well as the use of a considerable amount of input variables to the classifier algorithm, which covers spectral bands important for the study of crops, suggesting that methods which incorporate the spectral characteristics of plants are valuable for classifying different characteristics of plants in the field (Chicchón Apaza et al., 2019).

Notably, the application of classification procedures by machine learning is of fundamental importance in the agricultural sector, as it allows the analysis of increasingly complex and numerous data from different origins and sources, producing accurate and reliable results, with smaller risks of errors when properly applied and when performance analyses are performed (Osco et al., 2020). Thus, the results described in this study confirm the possibility of identifying areas subjected to different foliar chitosan applications by means of images obtained from RPAS and machine learning via random forest. Knowing the spatial distribution of areas with different management practices is essential for a proper understanding of the development of agricultural in the field, as well as for anticipating returns in productivity and profitability of crops. The advantage of identifying plants under leaf chitosan management with images based on RPAS is the fast, economical, and non-destructive way of monitoring agricultural crops. However, traditional agronomic methods should not be completely replaced but rather combined with new technologies and computational remote sensing techniques. Studies on the classification of plants with different management practices of foliar application of chitosan using the techniques presented in this study are not reported in the literature, indicating a need to model the presence of the biostimulant in coffee plants.

Conclusions

The results presented in this study showed that the random forest machine learning method, applied to individualized spectral bands and vegetation indices from multispectral images obtained by RPAS, offers an adequate approach to classify coffee cultivars subjected and not subjected to foliar application of chitosan. The model indicated that the spectral bands of the red edge and near infrared, both individually and in combination with vegetation indices, were quite efficient for the proposed classification.

Disclosure statement

No potential conflict of interest was reported by the author(s).

Funding

This work was supported by Federal University of Lavras (UFLA), the National Council for Scientific and Technological Development (CNPq - project 310186/2023-4), the Minas Gerais State Research Support Foundation (FAPEMIG - project APQ-00661-22), the Brazilian Agricultural Research Company - Coffee Research Consortium (EMBRAPA - project 10.18.20.041.00.00), the Coordination for the Improvement of Higher Education Personnel (CAPES - Finance Code 001), the Graduate Program in Agricultural Engineering (PPGEA/UFLA) and University of Firenze (UniFI).

ORCID

Gabriel Araújo e Silva Ferraz http://orcid.org/0000-0001-6403-2210
Giuseppe Rossi http://orcid.org/0000-0003-0211-9294

Data availability statement

All research data supporting this publication are directly available within the publication.

References

Abd El-Aziz, M. H., & Khalil, M. S. (2020). Antiviral and Antinematodal potentials of chitosan: Review. *Journal of Plant Science and Phytopathology*, *4*(2), 055–059. https://doi.org/10.29328/journal.jpsp.1001051

Barbosa, B. D. S., Ferraz, G. A. E. S., Costa, L., Ampatzidis, Y., Vijayakumar, V., & dos Santos, L. M. (2021). UAV-based coffee yield prediction utilizing feature selection and deep learning. *Smart Agricultural Technology*, *1*, 100010. https://doi.org/10.1016/j.atech.2021.100010

Barnes, M. L., Breshears, D. D., Law, D. J., Van Leeuwen, W. J., Monson, R. K., Fojtik, A. C., Moore, D. J. P., & Barron-Gafford, G. A. (2017). Beyond greenness: Detecting temporal changes in photosynthetic capacity with hyperspectral reflectance data. *PLOS ONE*, *12*(12), e0189539. https://doi.org/10.1371/journal.pone.0189539

Bausch, W. C., & Duke, H. R. (1996). Remote sensing of plant nitrogen status in corn. *Transactions of the ASAE*, *39*(5), 1869–1875. https://doi.org/10.13031/2013.27665

Behboudi, F., Tahmasebi Sarvestani, Z., Kassaee, M. Z., Modares Sanavi, S. A. M., Sorooshzadeh, A., & Ahmadi, S. B. (2018). Evaluation of chitosan nanoparticles effects on yield and yield components of barley (hordeum vulgare L.) under late season drought stress. *Journal of Water and Environmental Nanotechnology*, *3*(1), 22–39.

Bento, N. L., Ferraz, G. A. E. S., Barata, R. A. P., Soares, D. V., Santana, L. S., & Barbosa, B. D. S. (2022). Estimate and temporal monitoring of height and diameter of the canopy of recently transplanted coffee by a remotely piloted aircraft system. *AgriEngineering*, *4*(1), 207–215. https://doi.org/10.3390/agriengineering4010015

Bento, N. L., Ferraz, G., Amorim, J., Santana, L. S., Barata, R. A. P., Soares, D. V., & Ferraz, P. F. P. (2023). Weed detection and mapping of a coffee farm by a remotely piloted aircraft system. *Agronomy*, *13*(3), 830. https://doi.org/10.3390/agronomy13030830

Berger, L. R. R., Stamford, T. C. M., & Stamford, N. P. (2011). Perspectivas para o uso da quitosana na agricultura. *Revista Iberoamericana de Polímeros*, *12*(4), 195–215.

Breiman, L. (2001). Random forests. *Machine Learning*, *45*(1), 5–32. https://doi.org/10.1023/A:1010933404324

Buschmann, C., & Nagel, E. (1993). In vivo spectroscopy and internal optics of leaves as basis for remote sensing of vegetation. *International Journal of Remote Sensing*, *14*(4), 711–722. https://doi.org/10.1080/01431169308904370

Calou, V. B. C., dos Santos Teixeira, A., Moreira, L. C. J., Lima, C. S., de Oliveira, J. B., & de Oliveira, M. R. R. (2020). The use of UAVs in monitoring yellow sigatoka in banana. *Biosystems Engineering*, *193*, 115–125. https://doi.org/10.1016/j.biosystemseng.2020.02.016

Cao Qiang, C. Q., Miao YuXin, M. Y., Wang HongYe, W. H., Huang ShanYu, H. S., Cheng ShanShan, C. S., Khosla, R., & Jiang RongFeng, J. R. (2013). Non-destructive estimation of rice plant nitrogen status with crop circle multispectral active canopy sensor. *Field Crops Research*, *154*, 133–144. https://doi.org/10.1016/j.fcr.2013.08.005

Cao, Z., Yao, X., Liu, H., Liu, B., Cheng, T., Tian, Y., & Zhu, Y. (2019). Comparison of the abilities of vegetation indices and photosynthetic parameters to detect heat stress in wheat. *Agricultural and Forest Meteorology*, *265*, 121–136. https://doi.org/10.1016/j.agrformet.2018.11.009

Chen, J. (1996). Evaluation of vegetation indices and a modified simple ratio for boreal applications. *Canadian Journal of Remote Sensing*, *22*(3), 229–242. https://doi.org/10.1080/07038992.1996.10855178

Cheng, B., Pei, B., Wang, Z., & Hu, Q. (2017). Advances in chitosan-based superabsorbent hydrogels. *RSC Advances*, *7*(67), 42036–42046. https://doi.org/10.1039/C7RA07104C

Chicchón Apaza, M. Á., Monzón, H. M. B., & Alcarria, R. (2019). Semantic segmentation of weeds and crops in multispectral images by using a convolutional neural networks based on u-net. *International Conference on Applied Technologies* (pp. 473–485). Springer International Publishing, Cham.

Companhia Nacional de Abastecimento - CONAB. (2023). *Acompanhamento da Safra Brasileira de Café- Primeiro Levantamento* (Vol. 1). Boletim Safra; Observatório Agrícola.

Dash, J., & Curran, P. J. (2004). The MERIS terrestrial chlorophyll index. *International Journal of Remote Sensing*, *25*(23), 5403–5413. https://doi.org/10.1080/0143116042000274015

Dash, M., & Liu, H. (1997). Feature selection for classification. *Intelligent Data Analysis*, *1*(3), 131–156. https://doi.org/10.3233/IDA-1997-1302

De Almeida Furtado, L. F., Silva, T. S. F., & de Moraes Novo, E. M. L. (2016). Avaliação SAR de banda C de dupla estação e polarimétrica total para mapeamento de vegetação nas áreas úmidas de várzea amazônica. *Sensoriamento Remoto Meio Ambiente*, *174*, 212–222.

De Castro, L. N., & Ferrari, D. G. (2017). *Introdução à mineração de dados*. Saraiva Educação SA.

Feliziani, E., Landi, L., & Romanazzi, G. (2015). Preharvest treatments with chitosan and other alternatives to conventional fungicides to control postharvest decay of strawberry. *Carbohydrate Polymers*, *132*, 111–117. https://doi.org/10.1016/j.carbpol.2015.05.078

Fiorio, P. R., Coelho, R. D., Barros, P. P. S., Bonilla, M. M. Z., & Gady, A. P. B. (2018). Comportamento espectral de folhas da cana-de-açúcar na presença de déficit hídrico. *Irriga*, *23*(3), 609–621. https://doi.org/10.15809/irriga.2018v23n3p609-621

Gamon, J. A., & Surfus, J. S. (1999). Assessing leaf pigment content and activity with a reflectometer. *The New Phytologist*, *143*(1), 105–117. https://doi.org/10.1046/j.1469-8137.1999.00424.x

Gangireddygari, V. S. R., Chung, B. N., Cho, I. S., & Yoon, J. Y. (2021). Inhibitory effect of chitosan and phosphate cross-linked chitosan against cucumber mosaic virus and pepper mild mottle virus. *Plant Pathology Journal*, *37*(6), 632. https://doi.org/10.5423/PPJ.OA.10.2021.0155

Gislason, P. O., Benediktsson, J. A., & Sveinsson, J. R. (2006). Random forests for land cover classification. *Pattern Recognition Letters*, *27*(4), 294–300. https://doi.org/10.1016/j.patrec.2005.08.011

Gitelson, A. A., Viña, A., Arkebauer, T. J., Rundquist, D. C., Keydan, G., & Leavitt, B. (2003). Remote estimation of leaf area index and green leaf biomass in maize canopies. *Geophysical Research Letter*, *30*(5).

Haboudane, D. (2004). Hyperspectral vegetation indices and novel algorithms for predicting green LAI of crop canopies: Modeling and validation in the context of precision agriculture. *Remote Sensing of Environment*, *90*(3), 337–352. https://doi.org/10.1016/j.rse.2003.12.013

Hidangmayum, A., Dwivedi, P., Katiyar, D., & Hemantaranjan, A. (2019). Application of chitosan on plant responses with special reference to abiotic stress. *Physiology & Molecular Biology of Plants*, *25*(2), 313–326. https://doi.org/10.1007/s12298-018-0633-1

Huq, T., Khan, A., Brown, D., Dhayagude, N., He, Z., & Ni, Y. (2022). Sources, production and commercial applications of fungal chitosan: A review. *Journal of Bioresources & Bioproducts*, *7*(2), 85–98. https://doi.org/10.1016/j.jobab.2022.01.002

James, G., Witten, D., Hastie, T., & Tibshirani, R. (2013). *An introduction to statistical learning* (p. 112). New York: Springer.

Knipling, E. B. (1970). Physical and physiological basis for the reflectance of visible and near-infrared radiation from vegetation. *Remote Sensing of Environment*, *1*(3), 155–159. https://doi.org/10.1016/S0034-4257(70)80021-9

Kouadio, L., Deo, R. C., Byrareddy, V., Adamowski, J. F., Mushtaq, S., & Phuong Nguyen, V. (2018). Artificial intelligence approach for the prediction of robusta coffee yield using soil fertility properties. *Computers and Electronics in Agriculture*, *155*, 324–338. https://doi.org/10.1016/j.compag.2018.10.014

Kuhn, M., & Johnson, K. (2013). *Applied predictive modeling* (Vol. 26). New York: Springer.

Kumaraswamy, R. V. K., Kumari, S., Choudhary, R. C., Pal, A., Raliya, R., Biswas, P. V., & Saharan, V. (2018).

Engineered chitosan based nanomaterials: Bioactivities, mechanisms and perspectives in plant protection and growth. *International Journal of Biological Macromolecules*, *113*, 494–506. https://doi.org/10.1016/j.ijbiomac.2018.02.130

Le, T. S., Harper, R., & Dell, B. (2023). Application of remote sensing in detecting and monitoring water stress in forests. *Remote Sensing*, *15*(13), 3360. https://doi.org/10.3390/rs15133360

Liakos, K. G., Busato, P., Moshou, D., Pearson, S., & Bochtis, D. (2018). Machine learning in agriculture: A review. *Sensors (Switzerland)*, *18*(8), 2674. https://doi.org/10.3390/s18082674

Liu, H., Tian, W., Li, B., Wu, G., Ibrahim, M., Tao, Z., Wang, Y., Xie, G., Li, H., & Sun, G. (2012). Antifungal effect and mechanism of chitosan against the rice sheath blight pathogen, rhizoctonia solani. *Biotechnology Letters*, *34*(12), 2291–2298. https://doi.org/10.1007/s10529-012-1035-z

Lu, J., Miao, Y., Shi, W., Li, J., & Yuan, F. (2017). Evaluating different approaches to non-destructive nitrogen status diagnosis of rice using portable RapidSCAN active canopy sensor. *Scientific Reports*, *7*(1), 14073. https://doi.org/10.1038/s41598-017-14597-1

Mahdianpari, M., Salehi, B., Mohammadimanesh, F., & Motagh, M. (2017). Random forest wetland classification using ALOS-2 L-band, RADARSAT-2 C-band, and TerraSAR-X imagery. *ISPRS Journal of Photogrammetry & Remote Sensing*, *130*, 13–31. https://doi.org/10.1016/j.isprsjprs.2017.05.010

Mao, W., Wang, Y., & Wang, Y. (2003). *Real-time detection of between-row weeds using machine vision*. American Society of Agricultural and Biological Engineers.

Mariano, D., & Paz, F. J. (2020). *Data mining* (1 ed.). Sagah.

Marin, D. B., Ferraz, G. A. E. S., Guimarães, P. H. S., Schwerz, F., Santana, L. S., Barbosa, B. D. S., Barata, R. A. P., Faria, R. D. O., Dias, J. E. L., Conti, L., & Rossi, G. (2021). Remotely piloted aircraft and random forest in the evaluation of the spatial variability of foliar nitrogen in coffee crop. *Remote Sensing*, *13*(8), 1471. https://doi.org/10.3390/rs13081471

Marin, D. B., Ferraz, G. A. E. S., Santana, L. S., Barbosa, B. D. S., Barata, R. A. P., Osco, L. P., Ramos, A. P. M., & Guimarães, P. H. S. (2021). Detecting coffee leaf rust with UAV-based vegetation indices and decision tree machine learning models. *Computers and Electronics in Agriculture*, *190*, 106476. https://doi.org/10.1016/j.compag.2021.106476

Masjedi, M. H., Roozbahani, A., & Baghi, M. (2017). Assessment effect of chitosan foliar application on total chlorophyll and seed yield of wheat (Triticum aestivum L.) under water stress conditions. *Journal of Crop Nutrition Science*, *3*, 14–26. https://oiccpress.com/jcns/article/view/5866

Mehta, P., Bukov, M., Wang, C. H., Day, A. G. R., Richardson, C., Fisher, C. K., & Schwab, D. J. (2019). A high-bias, low-variance introduction to machine learning for physicists. *Physics Reports*, *810*, 1–124. https://doi.org/10.1016/j.physrep.2019.03.001

Meng, D., Garba, B., Ren, Y., Yao, M., Xia, X., Li, M., & Wang, Y. (2020). Antifungal activity of chitosan against aspergillus ochraceus and its possible mechanisms of action. *International Journal of Biological Macromolecules*, *158*, 1063–1070. https://doi.org/10.1016/j.ijbiomac.2020.04.213

Meyer, G. E., Hindman, T. W., & Lakshmi, K. (1998). Machine vision detection parameters for plant species identification. In G.E. Meyer & J.A. DeShazer (Eds.), *Precision Agriculture and Biological Quality*, *Proceedings of SPIE* (Vol. 3543, pp. 327–335). Bellingham, WA.

Osco, L. P., Júnior, J. M., Ramos, A. P. M., Furuya, D. E. G., Santana, D. C., Teodoro, L. P. R., Gonçalves, W. N., Baio, F. H. R., Pistori, H., Júnior, C. A. D. S., & Teodoro, P. E. (2020). Leaf nitrogen concentration and plant height prediction for maize using UAV-Based multispectral imagery and machine learning techniques. *Remote Sensing*, *12*(19), 3237. https://doi.org/10.3390/rs12193237

Pellá, M. C., Lima-Tenório, M. K., Tenório-Neto, E. T., Guilherme, M. R., Muniz, E. C., & Rubira, A. F. (2018). Chitosan-based hydrogels: From preparation to biomedical applications. *Carbohydrate Polymers*, *196*, 233–245. https://doi.org/10.1016/j.carbpol.2018.05.033

Perry, C. R., Jr., & Lautenschlager, L. F. (1984). Functional equivalence of spectral vegetation indices. *Remote Sensing of Environment*, *14*(1–3), 169–182. https://doi.org/10.1016/0034-4257(84)90013-0

Priya, R., & Ramesh, D. (2020). ML based sustainable precision agriculture: A future generation perspective. *Sustainable Computing: Informatics and Systems*, *28*, 100439. https://doi.org/10.1016/j.suscom.2020.100439

Qiu, J., Wu, Q., Ding, G., Xu, Y., & Feng, S. (2016). A survey of machine learning for big data processing. *EURASIP Journal on Advances in Signal Processing*, *2016*(1), 1–16. https://doi.org/10.1186/s13634-016-0355-x

Reglinski, T., Elmer, P. A. G., Taylor, J. T., Wood, P. N., & Hoyte, S. M. (2010). Inhibition of botrytis cinerea growth and suppression of botrytis bunch rot in grapes using chitosan. *Plant Pathology*, *59*(5), 882–890. https://doi.org/10.1111/j.1365-3059.2010.02312.x

Richardson, A. J., & Wiegand, C. L. (1977). Distinguishing vegetation from soil background information. *Photogrammetric Engineering and Remote Sensing*, *43*(12), 1541–1552.

Román-Doval, R., Torres-Arellanes, S. P., Tenorio-Barajas, A. Y., Gómez-Sánchez, A., & Valencia-Lazcano, A. A. (2023). Chitosan: Properties and its application in agriculture in context of molecular weight. *Polymers*, *15*(13), 2867. https://doi.org/10.3390/polym15132867

Rondeaux, G., Steven, M., & Baret, F. (1996). Optimization of soil-adjusted vegetation indices. *Remote Sensing of Environment*, *55*, 95–107. https://doi.org/10.1016/0034-4257(95)00186-7

Roujean, J. L., & Breon, F. M. (1995). Estimating PAR absorbed by vegetation from bidirec tional reflectance measurements. *Remote Sensing of Environment*, *51*(3), 375–384. https://doi.org/10.1016/0034-4257(94)00114-3

Rouse, J. W., Haas, R. H., Schell, J. A., & Deering, D. W. (1974). Monitoring vegetation systems in the great plains with ERTS. In S.C. Freden, E.P. Mercanti, & M. Becker (Eds.), *Third earth resources technology satellite-1 symposium. Volume I: Technical presentations, NASA SP-351* (pp. 309–317). NASA.

Santana, L. S., Ferraz, G. A. E. S., Santos, G. H. R. D., Bento, N. L., & Faria, R. D. O. (2023). Identification and counting of coffee trees based on convolutional neural network applied to RGB images obtained by RPA. *Sustainability*, *15*(1), 820. https://doi.org/10.3390/su15010820

Santos, L. M. D., Ferraz, G. A. E. S., Barbosa, B. D. S., & Andrade, A. D. (2020). Use of remotely piloted aircraft in precision agriculture: A review. *Dyna*, *86*(210), 284–291. https://doi.org/10.15446/dyna.v86n210.74701

Shanahan, J. F., Schepers, J. S., Francis, D. D., Varvel, G. E., Wilhelm, W. W., Tringe, J. M., Schlemmer, M. R., & Major, D. J. (2001). Use of remote-sensing imagery to estimate corn grain yield. *Agronomy Journal*, *93*(3), 583–589. https://doi.org/10.2134/agronj2001.933583x

Silveira, N. M., Seabra, A. B., Marcos, F. C., Pelegrino, M. T., Machado, E. C., & Ribeiro, R. V. (2019). Encapsulation of S-nitrosoglutathione into chitosan nanoparticles improves drought tolerance of sugarcane plants. *Nitric Oxide: Biology & Chemistry / Official Journal of the Nitric Oxide Society*, *84*, 38–44. https://doi.org/10.1016/j.niox.2019.01.004

Sripada, R. P., Heiniger, R. W., White, J. G., & Meijer, A. D. (2006). Aerial color infrared photography for determining early in-season nitrogen requirements in corn. *Agronomy Journal*, *98*(4), 968–977. https://doi.org/10.2134/agronj2005.0200

Tucker, C. J. (1979). Red and photographic infrared linear combinations for monitoring vegetation. *Remote Sensing of Environment*, *8*(2), 127–150. https://doi.org/10.1016/0034-4257(79)90013-0

Wang, F. M., Huang, J. F., Tang, Y. L., & Wang, X. Z. (2007). New vegetation index and its application in estimating leaf area index of rice. *Rice Science*, *14*(3), 195–203. https://doi.org/10.1016/S1672-6308(07)60027-4

Wu, W. (2014). The generalized difference vegetation index (GDVI) for dryland characterization. *Remote Sensing*, *6*(2), 1211–1233. https://doi.org/10.3390/rs6021211

Xing, D., & Wu, Y. (2012). Photosynthetic response of three climber plant species to osmotic stress induced by polyethylene glycol (PEG) 6000. *Acta Physiologiae Plantarum / Polish Academy of Sciences, Committee of Plant Physiology Genetics & Breeding*, *34*, 1659–1668. https://doi.org/10.1007/s11738-012-0961-7

Xing, K., Li, T. J., Liu, Y. F., Zhang, J., Zhang, Y., Shen, X. Q., & Qin, S. (2018). Antifungal and eliciting properties of chitosan against ceratocystis fimbriata in sweet potato. *Food Chemistry*, *268*, 188–195. https://doi.org/10.1016/j.foodchem.2018.06.088

Yang, Z., Willis, P., & Mueller, R. (2008, November). Impact of band-ratio enhanced AWIFS image to crop classification accuracy. *Proceedings of Pecora*, *17*(1), 1–11.

Zahid, N., Maqbool, M., Siddiqui, Y., Manickam, S., & Ali, A. (2015). Regulation of inducible enzymes and suppression of anthracnose using submicron chitosan dispersions. *Scientia Horticulturae*, *193*, 381–388. https://doi.org/10.1016/j.scienta.2015.07.014